

# DUAL WAVELENGTH EMISSION IN INJECTORLESS QUANTUM CASCADE LASERS

S. Katz, M. Maier, G. Boehm, M.-C. Amann  
Chair of Semiconductor Technology  
WSI  
85748 Garching, Germany  
katz@wsi.tum.de

**Abstract** — An injector-less quantum cascade laser is presented, which is capable of concurrent light emission at two different wavelengths (6.4 and 7.6  $\mu\text{m}$ ) at 77 K. The maximum operation temperature is 340 K and at 77 K the laser threshold current density is 0.19  $\text{kA}/\text{cm}^2$ . A competing approach using a single active zone for dual wavelength emission is also presented.

*Injectorless quantum cascade lasers, dual wavelength emission;*

## I. INTRODUCTION

By today, dual wavelength emission has been shown in quantum cascade lasers,<sup>[1][2]</sup> but not yet with an injectorless quantum cascade laser using a sequentially built-up active zone. The driving idea behind our different wavelength emitting cascade laser would be the THz emission at room temperature with a monolithically integrated device. The concept of this THz source would require a synthetic non-linear crystal, being pumped by two mid infrared lasers, for creating the THz wave by difference-frequency generation.<sup>[3]</sup> The key advantage of the injectorless quantum cascade laser in comparison to the injector based one, is the reduction of passive material in the active zone. An injectorless quantum cascade laser has approximately twice as much periods within the same thickness of the active zone. This provides enough stages for lasing even with a shared design of the active zone. Therefore we have designed an injectorless quantum cascade laser with two diverse periods, one emitting at 6.4  $\mu\text{m}$  and another one at 7.6  $\mu\text{m}$ . Additionally an injectorless quantum cascade laser is presented, which uses only one design inside its active zone for the dual emission, a design concept especially interesting for synthetic nonlinearities.

## II. THE DESIGN

### A. The Active Zone

For creating a dual wavelength emission, an active zone, including two diverse periods, had to be designed. The period emitting at 7.6  $\mu\text{m}$  had the following design: 3.0/1.9/2.2/**0.8**/6.0/1.1/4.4/**3.4** with the bold numbers being the  $\text{Al}_{0.56}\text{In}_{0.44}\text{As}$  barriers while the second period contained the

layer sequence: 2.8/1.4/1.2/**1.0**/6.5/**1.0**/5.0/1.3/4.0/**2.8** with the bold numbers being the  $\text{Al}_{0.635}\text{In}_{0.365}\text{As}$  barriers. In both sequences the Si-doping ( $5.2 \cdot 10^{16} \text{ cm}^{-3}$ ) is indicated by an underline, resulting into a doping sheet density of  $5.6 \cdot 10^{10} \text{ cm}^{-2}$  and of  $5.0 \cdot 10^{10} \text{ cm}^{-2}$ , respectively. The well material being used for both designs was an identical  $\text{Ga}_{0.4}\text{In}_{0.6}\text{As}$  alloy. For enabling a proper charge transition between each period, the active zone was built up with 60 periods of sequence one followed by 40 periods of sequence two resulting in an overall thickness of 2.45  $\mu\text{m}$ . Fig 1 shows the two diverse layer sequences, both lasing at a field of 98  $\text{kV}/\text{cm}$ .

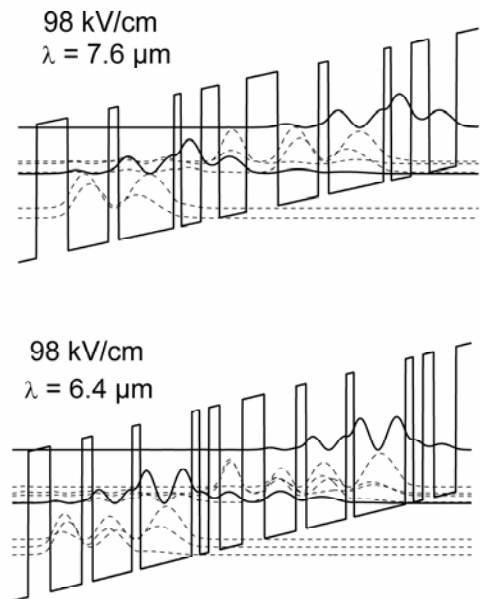


Figure 1. Bandstructure of layer sequence 1 & 2

An alternative approach, using a single active zone for the dual emission was also designed, which contains five different material compositions analogically to a regular injectorless quantum cascade laser presented in reference 5. Figure 2 shows the band structure of the alternative design approach, which contains the following material compositions:  $\text{AlAs}$ ,  $\text{Al}_{0.635}\text{In}_{0.365}\text{As}$ ,  $\text{Al}_{0.16}\text{Ga}_{0.31}\text{In}_{0.53}\text{As}$ ,  $\text{Ga}_{0.4}\text{In}_{0.6}\text{As}$  and  $\text{InAs}$ . The dipole matrix elements of the two possible optical transitions

are 1.0 nm and 1.2 nm, while the upper life time was calculated to 1.9 ps for an applied field of 85 kV/cm. For emptying the lower laser levels two additional energy levels were implemented, both located about the phonon energy below.

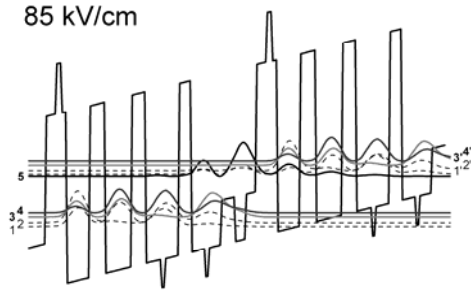


Figure 2. Band structure of the alternative approach, wavelengths are calculated to 7.6  $\mu\text{m}$  and 6.8  $\mu\text{m}$ , the optical transition occurs between level 5 to 4 and 5 to 3.

### B. The Waveguide

As wafer a n+ InP wafer was used and covered by a 3.3  $\mu\text{m}$  thick InP Buffer ( $6.0 \cdot 10^{16} \text{ cm}^{-3}$  Si-doped), a lattice matched 0.5  $\mu\text{m}$  strong GaInAs cladding followed before the active zone was epitaxially deposited. The top waveguide consisted of another cladding, identically to the one below the active zone, an InP waveguide of 2.5  $\mu\text{m}$  ( $6.0 \cdot 10^{16} \text{ cm}^{-3}$  Si-doped). The top contact was formed of another 0.8  $\mu\text{m}$  strong lattice matched GaInAs ( $5.0 \cdot 10^{18} \text{ cm}^{-3}$  Si-doped) cladding and the ohmic contact layer (0.2  $\mu\text{m}$ , lattice matched GaInAs,  $1.0 \cdot 10^{19} \text{ cm}^{-3}$  Si-doped). Figure 3 shows the simulated mode distribution in the waveguide for both wavelengths. The confinement factor  $\Gamma$  for the 6.4 (7.6)  $\mu\text{m}$  wave results in 0.31 (0.39) for the 40 (60) periods of the active zone.

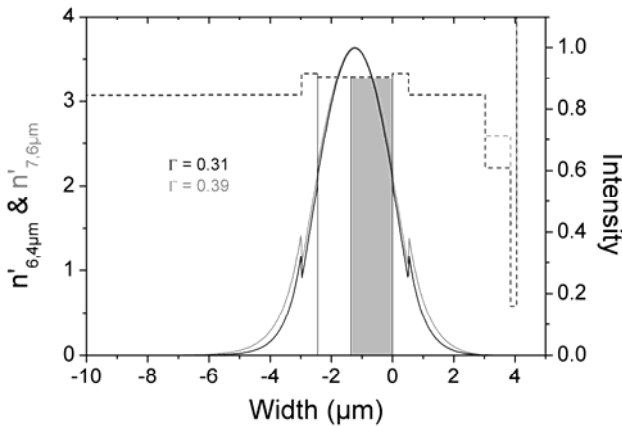


Figure 3. Mode distribution for the 6.4  $\mu\text{m}$  (black) and 7.6  $\mu\text{m}$  (grey) wave. The refractive index are also displayed (dashed) for the setup, from substrate (left) to top contact (right).

The waveguide design of the alternative approach was identical, but contained only 60 periods of the active zone design with a thickness of 1.63  $\mu\text{m}$  and a sheet doping density of  $1.6 \cdot 10^{11} \text{ cm}^{-2}$  per period.

### C. The Fabrication

The laser mesas were wet chemically etched using  $\text{HBr}:\text{H}_2\text{O}_2:\text{H}_2\text{O}$  (10:1:30), covered by a 350 nm strong insulating silicon dioxide layer. The top contact was formed by removing the silicon dioxide with PECVD etching and depositing Ti/Pt/Au contact pads. Finally the lasers were

thinned and a backside contact added. The widths of the laser mesas were roughly 18, 22 and 26 in  $\mu\text{m}$ .

## III. DEVICE CHARACTERISTICS

For the pulsed measurement a liquid-nitrogen-cooled and temperature controlled cryostat and a calibrated HgCdTe photovoltaic detector were used. The pulses were created with a high power pulse source, 0.2 to 1.0  $\mu\text{s}$  of duration, being repeated every 250 Hz to 10 kHz. The samples were setup on a copper heat sink, connected with a Sn-annealed Au-contact. For measuring the spectrum, two different methods, both using a Vertex70 (from Bruker), were applied. For the spectrum at different temperatures a regular FTIR spectroscopy measurement was done with a high repetition rate of pulses, while the time resolved measurements required a Step-Scan setup. The measurement setup required a KBr beam splitter, another liquid nitrogen cooled HgCdTe detector and of course some Au-plated mirrors.

### A. Shared Design

Figure 4 shows the output power & voltage vs. the current density for a sample 4 mm long and 22  $\mu\text{m}$  wide at different temperatures. The threshold current density at 77 K was measured with 0.19  $\text{kA/cm}^2$  increasing to 1.7  $\text{kA/cm}^2$  for 300 K, comparable to other injectorless quantum cascade lasers.<sup>[5][6][7]</sup> From the temperature dependent behavior of the threshold current density a  $T_0$  of 130 K was estimated. The maximum temperature for dual wavelength emission was determined with 250 K, while single wave emission worked up to 340 K. The threshold field strength is 94 kV/cm at 77 K and 91 kV/cm at 300 K. An explanation of this is already given by M. Wanke and Co in 2001 with their injectorless quantum cascade laser.<sup>[8]</sup>

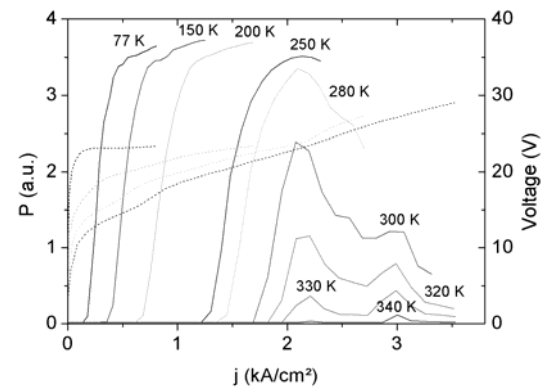


Figure 4. current density vs. output power (solid) and voltage for different temperatures for a 4 mm long and 18  $\mu\text{m}$  wide laser

Bearing in mind the possible application for a THz source, the emitted spectrum is particularly investigated. Figure 5 shows the spectra for 77 & 250 K. At 77 K the two emitted wavelengths are 6.39  $\mu\text{m}$  and 7.64  $\mu\text{m}$  corresponding to energy of 194 meV and 162 meV. At 250 K both wavelengths experience a red shift towards 6.53  $\mu\text{m}$  (190 meV) and 7.83  $\mu\text{m}$  (158 meV). The difference energy remains at 32 meV (39  $\mu\text{m}$ ), a quite unsuitable range considering phonon absorption.

The energy difference of the two emitted wavelengths was investigated during a pulse, using a time resolved step scan method. The results of this measurement are show in figure 6, where the energy difference of the two peak wavelengths is displayed over time in pulse at a current density of 0.68  $\text{kA/cm}^2$ .

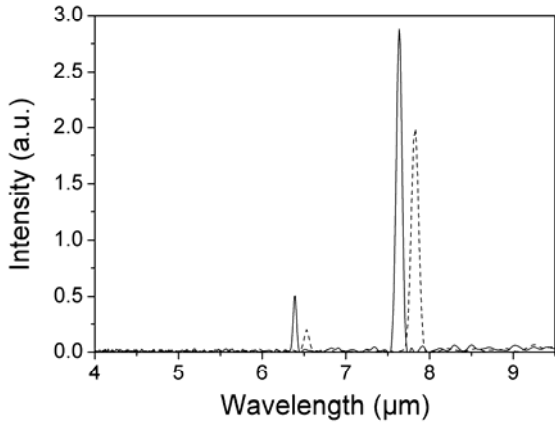


Figure 5. Spectrum of dual emission at 77 K (solid) & 250 K (dashed), the peak wavelengths are 6.39 and 7.64  $\mu\text{m}$  for 77 K and 6.53  $\mu\text{m}$  and 7.83  $\mu\text{m}$  for 250 K

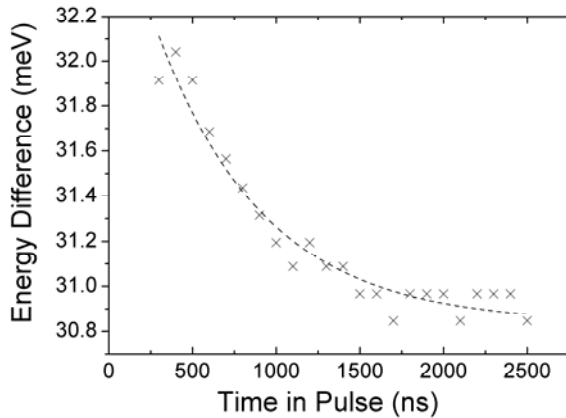


Figure 6. Energy difference of the dual emission peak wavelengths during a pulse. The dashed line displays an exponential fit ( $t_0 = 640$  ns).

### B. Alternative Approach

Finally the spectrum of the alternative approach was investigated. With the high doping and the low dipole matrix elements the current threshold density was high as expected, yielding  $3.5 \text{ kA/cm}^2$  at 77 K. The spectrum of the dual emission using only one active zone is displayed in figure 7 at a current density of  $4.7 \text{ kA/cm}^2$ . The two wavelengths differ from the simulated and expected value roughly by 5 %.

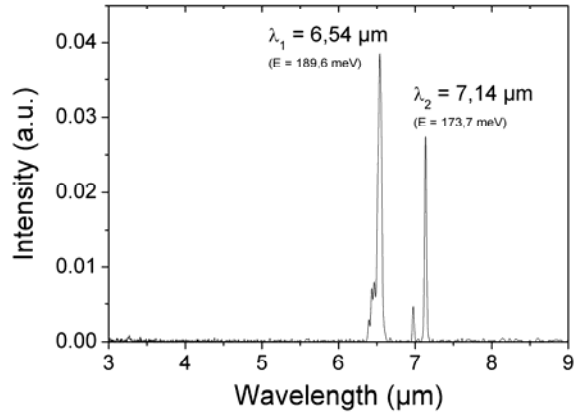


Figure 7. Spectrum of dual emission in alternative approach at 77 K and  $4.7 \text{ kA/cm}^2$ . The energy difference is 16 meV, corresponding to 78  $\mu\text{m}$  considering the difference frequency generation.

## IV. CONCLUSION

We have shown that a possible mid infrared pump source for THz Emission could be based on injectorless quantum cascade lasers. Their main advantage arises from their reduced length of the active zone in comparison to the injector based quantum cascade lasers. For ensuring a more simple integration into a single device, the shared active zone design is strongly recommended instead of the alternative approach. The dual emission demonstrated here lies at unsuitable  $6.4 \mu\text{m}$  and  $7.6 \mu\text{m}$  but the laser still operates at low threshold current densities of  $1.7 \text{ kA/cm}^2$  at room temperature and  $0.19 \text{ kA/cm}^2$  at 77 K.

## ACKNOWLEDGMENT

This work was in part supported by the “Nanosystems Initiative Munich” (NIM). The authors would like to thank for the support.

## REFERENCES

- [1] K. J. Franz, D. Wasserman, A. J. Hoffman, D. C. Jangraw, K.-T. Shiu, S. R. Forrest and C. Gmachl, “Evidence of cascaded emission in a dual-wavelength quantum cascade laser”, *Appl. Phys. Lett.*, vol. 90, 091104, 2007.
- [2] D. Qu, F. Xie, G. Shu, S. Momen, E. Narimanov and C. Gmachl, “Second-harmonic generation in quantum cascade lasers with electric field and current dependent nonlinear susceptibility”, *Appl. Phys. Lett.*, vol. 90, 031105, 2007.
- [3] M. Belkin, et. al., “Terahertz quantum-cascade-laser source based on intracavity difference-frequency generation” *Phot. Letters*, vol. 1, pp. 288–292, May 2007.
- [4] S. Katz, G. Boehm and M.-C. Amann, “Low-threshold Injectorless Quantum Cascade Laser with four material compositions”, unpublished
- [5] A. Friedrich, G. Scarpa, G. Boehm and M.-C. Amann, “High performance injectorless quantum cascade lasers”, *Elec. Lett.*, 41, 2005.
- [6] A. Friedrich, C. Huber, G. Boehm and M.-C. Amann, “Low threshold room-temperature operation of injectorless quantum cascade lasers: influence of doping density”, *Elec. Lett.*, 42, 2006.
- [7] S. Katz, A. Friedrich, G. Boehm, M.-C. Amann, „Continuous wave operation of injectorless quantum cascade lasers at low temperatures“, in press
- [8] M. Wanke, F. Capasso, C. Gmachl, “Injectorless Quantum cascade laser”, *Appl. Phys. Lett.*, vol. 78., pp. x1-x2., 2001.